Research article

Synthesis, characterization of Ca $(OH)_2$: TiO_2 nanocomposite and evaluation of its antimicrobial efficacy

Jenan Hussein Taha

Physiology Department, College of Medicine, University of Al- Nahrain, Baghdad, Iraq

(Received: August 2023 Revised: September 2023 Accepted: October 2023)

Corresponding author: **Jenan Hussein Taha**. Email: asjenan@gmail.com

ABSTRACT

Introduction and Aim: Root canal treatment is a dental operation that entails the extraction of the compromised tooth pulp tissue, sterilization of the root canal system, and subsequent filling with an inert substance. To mitigate the potential for bacterial infections and subsequent difficulties, it is customary for patients to receive a prescription for antibiotics prior to undergoing a root canal procedure. The objective of this study was to assess the effectiveness of $Ca(OH)_2$: TiO_2 nanoparticles as a potential substitute for antibiotics in root canal therapies, while also investigating their antibacterial properties against specific infections.

Materials and Methods: Ca $(OH)_2$: TiO_2 nanoparticles were synthesized chemically using calcium hydroxide and varying concentrations of titanium oxide powder by a sol-gel process. The Ca $(OH)_2$: TiO_2 nanoparticles synthesized was characterized using Field Emission Scanning Electron Microscope (FE-SEM), energy dispersive X-ray (EDX), Fourier Transform Infrared Spectrometer (FT-IR), and UV-Vis spectrophotometry. The antibacterial activity of the synthesized nanoparticles was evaluated against pathogens *Escherichia coli*, *Staphylococcus aureus,* and *Candida albicans spp.*) by gel diffusion method.

Results: FE-SEM analysis indicated that the Ca $(OH)_2$: TiO_2 composite material exhibited an amorphous structure, characterized by a particle size measuring 25.88 nm. But FTIR was focused on the spectral region between 4000 and 450 cm-1. The absorption spectra of nanoparticles composed of titanium dioxide consistently displayed a prominent peak at a wavelength of 300 nm. The results of the experiment pertaining to the biological effects of composites suggest that the inclusion of TiO2 nanoparticles at concentrations of 25%, 50%, and 75% in the composite material led to a notably wider inhibitory zone in comparison to the use of $Ca(OH)_2$ alone, with a statistically significant p-value of 0.05.

Conclusion: The use of varying concentrations of Ca $(OH)_2TiO_2$ improves microbial activity against *Escherichia coli, Staphylococcus, and Candida*.

Keywords: Root canal treatment; calcium hydroxide; titanium oxide; Ca $(OH)_2TiO_2$ nanoparticles.

INTRODUCTION

Multiple studies have demonstrated that the presence of bacteria within the root canal has a significant impact on the stability, development, and production of root lesions when root canal therapy is being performed. This has been shown to be the case in situations when bacteria are present (1-3). Antibacterial agents are commonly employed for the purpose of root canal disinfection, mostly owing to the intricate and constricted nature of the root canal system, as well as the challenges associated with adequately preparing the area to effectively eliminate bacterial infections (4). Despite the administration of pharmaceutical substances, certain strains of bacteria may exhibit resilience, leading to their proliferation and subsequent colonization inside the targeted region (5). The resolution of this issue is commonly achieved through the utilization of calcium hydroxide, a mineral antibacterial substance, to fill the channel between treatments (6). The use of calcium hydroxide is widespread; however, research has indicated that the antibacterial activity of calcium hydroxide can be impeded by the various components present in dentine (7).

The effectiveness of calcium hydroxide can be improved by combining it with nanoparticles, according to the findings of several researches that have been conducted on the topic. This combination has the potential to act as a treatment for root canal infections, which would eliminate germs (8, 9). Nanomaterials have a large surface area, the ability to pass through the cytoplasmic barrier of bacterial cell walls, which ultimately results in the death of the bacteria, and a low incidence of side effects (10–12). These factors contribute to the nanomaterials' remarkable effectiveness in the fight against bacterial diseases. The major purpose of this research was to produce and analyze a calcium hydroxide and titanium oxide composite nanoparticle, which we will refer to as $Ca(OH)_2$:TiO_2 NP. Following that, the effectiveness of this composite nanoparticle was evaluated against several different bacterial infections, such as *Staphylococcus*, *Escherichia coli*, and *Candida spp.*

MATERIALS AND METHODS

Chemical synthesis of TiO_2 NPs

The chemical synthesis of calcium hydroxide titanium dioxide nanoparticles (TiO NPs) was conducted by a sol-gel technique, utilizing Ca $(OH)_2$ and TiO_2 powder as precursor materials (13-15). Different quantities of nanoparticles were generated by utilizing varying percentages (25, 50, 75) of TiO_2 powder. To provide a summary, the powders were combined with distilled water to produce a gel, which was then subjected to agitation at a temperature of 80 °C for a period of two hours. After this step, the gel was dried at a temperature of 70 °C for a duration of twenty hours, which resulted in the development of a powdery substance. A sintering process was carried out on the powder at a temperature of 1100 °C for a period of two hours. After a string of processes that came one after the other, the granules were sintered some more at a temperature of one thousand degrees Celsius (16-17).

Characterization of $Ca(OH)_2TiO_2$ nanoparticles

The characterization method involved the utilization of various analytical instruments, (FE-SEM), (EDX, (FTIR), and UV-Vis spectrophotometry. These instruments were employed to analyze and assess the properties of the samples that were developed. To examine the optical characteristics of the $Ca(OH)_2$:TiO_2 nanoparticles synthesized, an ultraviolet-visible spectrophotometer (UV2300 II, manufactured in Japan) was employed. In this study, we employed a field emission scanning electron microscope (FE-SEM) manufactured by JEOL India Pvt. Ltd., located in Delhi, India, as well as a Fourier transformed infrared (FTIR) spectrometer model 670 FTIR from the United States. These instruments were utilized to examine the characteristics of the nanoparticles that were generated, as well as to investigate the chemical bonds present between the constituent components.

Antimicrobial testing

The gel diffusion method was utilized to evaluate the antibacterial properties of the nanoparticles that were created. The purpose of this study was to determine how efficient the nanoparticles were against pathogenic microbes. Several potentially dangerous bacterial strains were tested using the Mueller-Hinton agar medium to determine the efficiency of an inhibitory agent. The three indicator microorganisms, namely *Escherichia coli*, *Staphylococcus aureus*, and *Candida albicans* spp., were initially cultivated in nutritional broth. Subsequently, the suspension containing a concentration range of 1.5 × 106 - 1.5×108 CFU/ml was plated onto Mueller-Hinton agar plates. A volume of 100 µL of the suspension containing $Ca(OH)_2$:TiO_2 nanoparticles was introduced into the 6mm deep wells on a plate. To encourage the growth of bacterial and fungal species, the plates were incubated at a temperature of 37 °C for a total of 24 and 48 hours, respectively. This was done with the specific intention of fostering population growth. The procedure for calculating the diameter (in millimeters) of the inhibitory zone was carried out in accordance with the approach described in other research investigations (18, 19).

RESULTS

To determine the particle size of the produced nanoparticles, the pictures obtained using (FE-SEM) were analyzed with the "Image J" program. Figs. 1a, 1b, and 1c show, respectively, the FESEM images of $Ca(OH)_2$:TiO_2 at varying percent concentrations of TiO_2 (25, 50, and 75). The crystal and amorphous morphologies of the Ca(OH)2:25% TiO2 can be seen in the FESEM images (Fig. 1a). The chemical production of TiO_2 nanoparticles, which have an amorphous and varied appearance, is depicted in Figs. 1b and 1c. The computed particle size for the three distinct concentrations of TiO_2 NPs was, in order from smallest to largest, 59.09, 33.58, and 24.87 nm, respectively.

The electron dispersive X-ray (EDX) spectra that were obtained from the samples that included $Ca(OH)_2$:TiO_2 are displayed in Figs. 2a, 2b, and 2c respectively. On the labels of the samples that are prepared, the names of the components as well as the amounts of those components in relative terms are printed. It was discovered that the samples contained titanium (Ti), calcium (Ca), and oxygen (O), although the presence of any contaminants was below the detection threshold of the energy-dispersive X-ray spectroscopy (EDX). Titanium (Ti), calcium (Ca), and oxygen (O) are all present in the samples without a shadow of a doubt. Fig. 2a depicts the elemental percentage of $Ca(OH)_2$:50% TiO_2, and Fig. 2b displays the results of Ca(OH)2:50% TiO2. In addition to the components of $Ca(OH)_2$, the presence of TiO2 (Ti, O) can be detected in all three samples, as illustrated in Fig. 2c. This can be seen alongside the existence of $Ca(OH)_2$ components. This component may be discovered in each of the three samples.

The Fourier Transformed Infrared (FTIR) spectra of the composite material consist of calcium hydroxide (Ca $(OH)_2$) and titanium dioxide (TiO_2). In the mode of diffuse reflection, the spectral range of the wave number extends from 4000 to 450 cm^{-1}. The absorption bands located in the higher frequency range were seen at 3641.60 cm^{-1} for the sample $Ca(OH)_2$:25% TiO_2, at 2924.09 cm^{-1} for the sample $Ca(OH)_2$:50% TiO_2, and for the sample $Ca(OH)_2$:75% TiO_2, as illustrated in Figs. 3a, 3b, and 3c respectively.

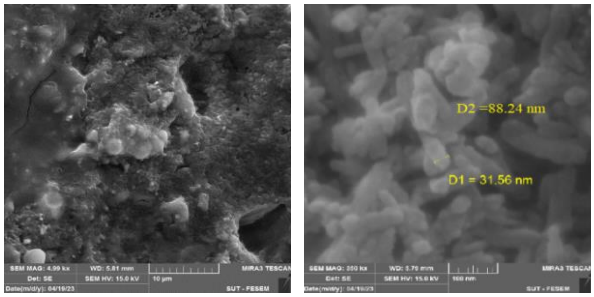

Fig 1a

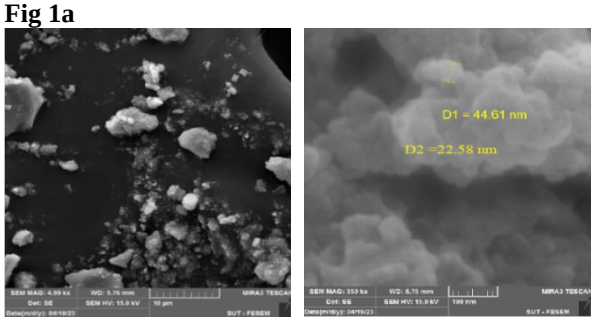

Fig 1b

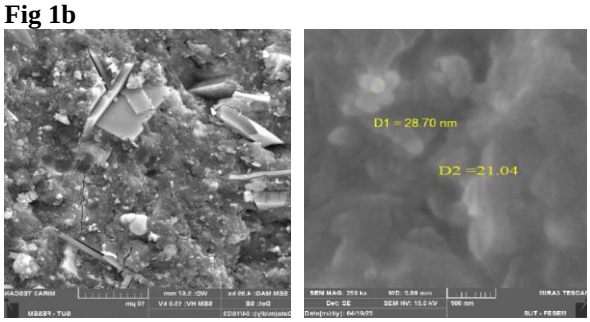

Fig 1c

Fig.1: The FESEM images of the (**a**) $Ca(OH)_2$:25% TiO_2, (b) $Ca(OH)_2$:50% TiO_2, and (**c**) $Ca(OH)_2$:75%TiO_2.

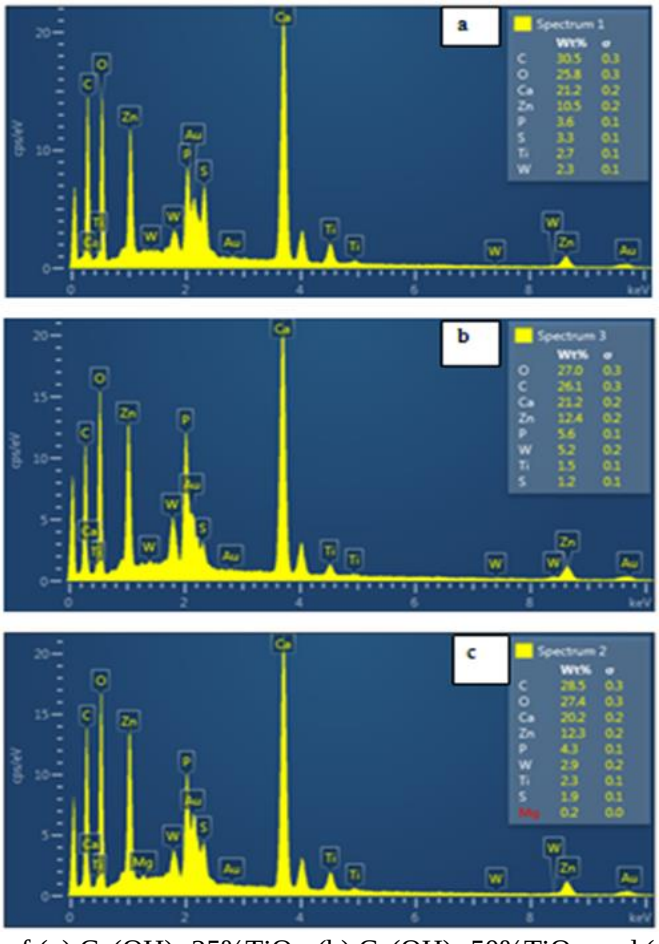

Fig 2: EDX diagrams of (**a**) $Ca(OH)_2$:25%TiO_2, (b) $Ca(OH)_2$:50%TiO_2, and (**c**) $Ca(OH)_2$:75%TiO_2.

The presence of these notable peaks can be ascribed to the elongation and oscillation of the hydroxyl group (OH). The wavenumbers of the detected peaks in the three samples are 3298.28, 2924.09, 2854.65, 2298.65, 2298.28, and 2864.65 cm^{-1}. These peaks can be attributed to the vibrational modes of the CH functional group. The wavenumbers 1730.08, 1666.50, 1600.92, 1534.05, 1597.09, and 1597.06 cm^{-1} were utilized for the purpose of characterizing the functional groups of (C=O) amines by the analysis of absorption bands. The detected peaks located at positions (1469.75, 1391.31, 1257.59, 1219.01, and 1469.67) cm^{-1} are ascribed to the three samples containing calcium and titanium, respectively. The observed peaks can be attributed to the deformation of (-C-H-) functional groups at the (C-O) bond, as well as the vibrational band located within the infrared spectrum at coordinates (1152.29, 1068.56, and 1033.85) cm^{-1}. The wavenumbers of 860.25 cm^{-1}, 806.25 cm^{-1}, and 813.96 cm^{-1} correspond to the vibrational bands attributed to C-H bonding. Nevertheless, it is important to acknowledge that the band was not observed in the experimental analysis of TiO2 nanoparticles. The vibrational frequencies associated with the (O-H) functional groups are closely approximated by the observed peaks at 759.95 cm^{-1}, 709.80 cm^{-1}, 798.53 cm^{-1}, 756.10 cm^{-1}, 706.95 cm^{-1}, and 601.79 cm^{-1}, as well as 799.95 cm^{-1} and 601.80 cm^{-1}. The peaks seen at wavenumbers 563.21 cm^{-1}, 416.62 cm^{-1}, and 567.07 cm^{-1} can be ascribed to the stretching vibration of the (Ti-O) band, as documented by (20-23).

UV-visible spectroscopy is a technique that is commonly recognized as being particularly effective for exploring the optical features of various materials, with a particular emphasis on semiconductors and nanomaterials. This is because the technique can observe wavelengths that are invisible to the human eye. The spectra of absorption for each of these three distinct compositions are shown in the demonstrated fig. They are as follows: $Ca(OH)_2$:25% TiO_2, $Ca(OH)_2$:50% TiO_2, and $Ca(OH)_2$:75% TiO_2. $Ca(OH)_2$:25% TiO_2 and $Ca(OH)_2$:50% TiO_2 both produced peaks at a wavelength of 210 nm, which was the wavelength at which the peaks were seen. On the other hand, the peak was found at a somewhat longer wavelength of 220 nm for the sample $Ca(OH)_2$:75% TiO_2 (Fig. 4).

The average diameter of the inhibitory zone is shown in Figure 5 and Table 1 for $Ca(OH)_2$:TiO_2 and TiO_2 at three different weight percent concentrations: 25, 50, and 75. The introduction of TiO_2 nanoparticles (NPs), in a broader sense, demonstrates a positive effect by increasing the inhibitory area. According to the findings, the different groups all display varying degrees of alterations in the amount of inhibition that may be noticed in their respective environments.

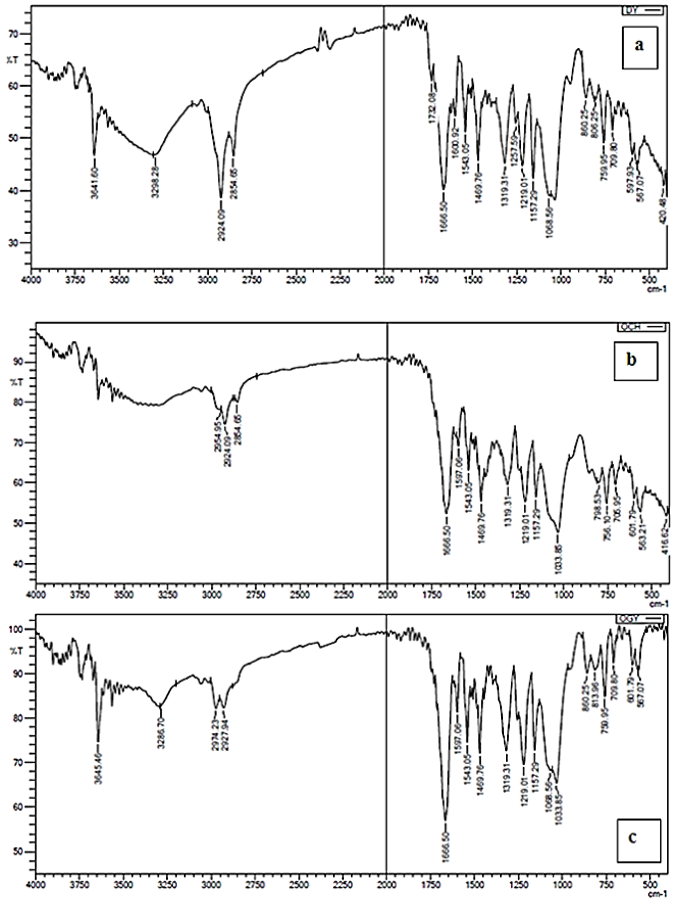

Fig. 3: FTIR spectra for (**a**) $Ca(OH)_2$:25% TiO_2, (b) $Ca(OH)_2$:50% TiO_2, and (**c**) $Ca(OH)_2$:75% TiO_2.

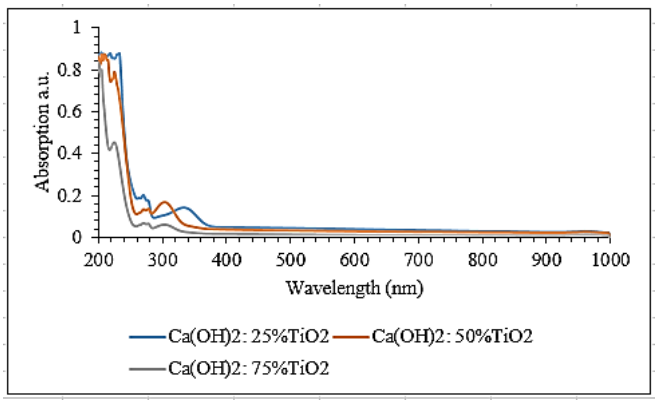

Fig. 4: UV-visible spectra of $Ca(OH)_2$: TiO_2

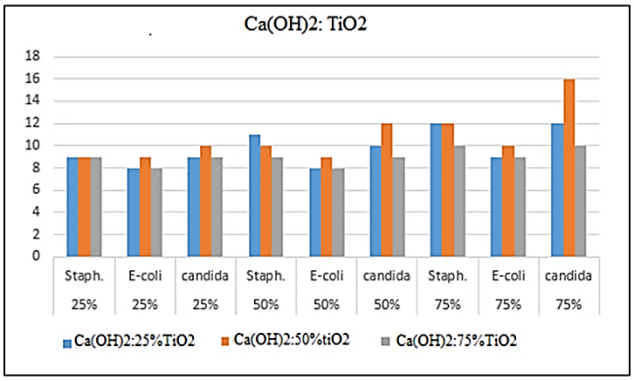

Fig. 5: The inhibitory zone histogram at varying $Ca(OH)_2$:TiO_2 concentrations

Table 1: The inhibition zone of $Ca(OH)_2$:TiO2.

Bacterial	0.07 g/ml			0.05 g/ml			0.02 g/ml		
	E.coli	***Staph***	***Candida***	***E.coli***	***Staph***	***Candida***	***E.coli***	***Staph***	***Candida***
$Ca(OH)_2$:25%TiO_2	9	12	12	8	11	10	8	9	9
$Ca(OH)_2$:50%TiO_2	10	12	16	9	10	12	9	9	10
$Ca(OH)_2$:75%TiO_2	9	10	10	8	9	9	8	9	9
p-value	0.0699	0.07423	0.00009	0.05598	0.07999	0.07014	0.07113	1	0.06997

DISCUSSION

The findings from the field emission scanning electron microscopy (FE-SEM) analysis revealed a correlation between the proportions of TiO_2 and the dimensions of the particles. To provide greater precision, a decrease in particle size was noted as the concentration of TiO_2 increased. The observed behavior can be attributed to a contact occurring between particles composed of titanium oxide and calcium hydroxide, alongside a disparity in the sizes of the respective ions engaged in the process (19). It is possible to draw the conclusion, based on the findings obtained from the EDX study, that there are no significant contaminants present. The absence of resistance in the raw materials that were utilized may be responsible for the presence of any pollutants that already exist. On the other hand, it is essential to keep in mind that the influence of these contaminants is negligible because of the precautions that were taken during the study process. This outcome further substantiates the materials that were developed for the research in terms of their trustworthiness as well as their suitability. The findings of this investigation allow for the inference to be made that the observed peaks within the wavelength range of (4000-450) cm-1 indicate the likely existence of functional groups such as C-O, -C-H-, and -OH. This conclusion may be reached based on the findings acquired from this study. These functional groupings that have been found are able to be related with the processing that occurs during the reaction (20). The absorption peak at a wavelength of 300 nm was observed, consistent with the findings reported in a previous study (23). The SEM image also provides evidence for the claim by revealing the presence of smaller particles. Furthermore, it provides data indicating that the unidirectional disappearing pattern of nanoparticle distribution is attributed to the increased adsorption of $Ca(OH)_2$:TiO_2 nanoparticles (24). According to the findings presented in Table 1, there appears to be a clear correlation between the amounts of TiO_2 present and the size of the inhibitory zone produced by each of the bacterial strains that were tested. Statistically there were significant variations in the diameter of the inhibitory zone for each of the selected bacteria when $Ca(OH)_2$:TiO_2 was present ($p > 0.05$), these findings are presented in the Table 1 which indicates that the incorporation of titanium dioxide nanoparticles (NPs) into a calcium hydroxide ($Ca(OH)_2$) solution results in improved resistance against bacteria, as indicated by an observed

enlargement in the diameter of the zone of inhibition. It is worth mentioning that the sample containing a concentration of TiO_2 at 7% demonstrated the most significant diameter of the inhibition zone, suggesting the highest degree of inhibition (25).

CONCLUSION

Within the limits of the current investigation, it can be concluded that the $Ca(OH)_2$:TiO_2 NPs improved the antagonism of Gram-negative *Escherichia coli*, Gram-positive *Staphylococcus aureus*, and *Candida albicans*. and therefore, could be used as an alternative to antimicrobials in root canal treatments.

CONFLICT OF INTEREST

The authors declare no conflicts of interest.

REFERENCES

1. Yousefshahi, H., M. Aminsobhani, M. Shokri, R. Shahbazi, Antibacterial properties of calcium hydroxide in combination with silver, copper, zinc oxide or magnesium oxide. Eur J Transl Myol. 2018; 28(3):274-279.
2. Rasheed, Z. Water temperature effect on hardness and flexural strength of (PMMA/TiO2 NPs) for dental applications. Baghdad Sci. J. 2022;19(4): 922-923.
3. Al-Saidi, M., Al-Bana, R.J.A., Hassan, E., AL-Rubaii, B.A.L., Extraction and characterization of nickel oxide nanoparticles from hibiscus plant using green technology and study of its antibacterial activity. Biomedicine. 2022; 42(6):1290-1295.
4. Jalil, I.S., Mohammad, S.Q., Mohsen, A.K., Al-Rubaii, B.A.L., Inhibitory activity of *Mentha spicata* oils on biofilms of *Proteus mirabilis* isolated from burns. Biomedicine. 2023; 43(02):748-752.
5. Byström, A., Sundqvist, G. Bacteriologic evaluation of the efficacy of mechanical root canal instrumentation in endodontic therapy; Scand J Dent Res. 1981; 89:321-328.
6. Tanomaru Filho, M., Leonardo, M., da Silva, L. Effect of irrigating solution and calcium hydroxide root canal dressing on the repair of apical and periapical tissues of teeth with the periapical lesion. J Endod. 2002;28:295-299.
7. Portenier, I., Haapasalo, H., Rye, A., Waltimo, T. Haapasalo, Inactivation of root canal medicaments by dentine, hydroxylapatite and bovine serum albumin. Int Endod J. 2001; 34:184-188.
8. Afkhami, F., Pourhashemi, S., Sadegh, M., Salehi, Y., Fard, M. Antibiofilm efficacy of silver nanoparticles as a vehicle for calcium hydroxide medicament against *Enterococcus faecalis*. J Dent. 2015; 43:1573-1579.
9. Javidi, M., Afkhami, F., Zarei, M., Ghazvini, K. Efficacy of a combined nanoparticulate/calcium hydroxide root canal medication on elimination of *Enterococcus faecalis*. Aust Endod J. 2014; 40:61-65.
10. Saifaldeen, A. K and Entisar, V. Exciting new nanocomposite using the solar energy to remove BG dye pollutants from wastewater. 2nd International Conference in Physical Science and Advanced Materials AIP Conf. 2021, Proc. 2372; 100007-1–100007-8.
11. Abass, E, Sondos, Zair, K. Thamera Mohammud, A. Saga Nagem, Recovery of pure hesperidin from Iraqi sweet oranges peel and study the effect in some bacteria. J. Baghdad for Sci.2014; 11(2):145-155.
12. Abdullah, A., Fayyadh, A. Fadhel Essa, S. Shammon Batros, Z. Studying the crystal structure, topography, and antibacterial of a novel Titania (TiO2NPs) prepared by a sol-gel manner. Baghdad Sci. J. 2019; 16 (4)78-86.
13. Jha, S., Singh, R., Pandey, A., Bhardwaj, M., Tripathi, S., Mishra, R. Bacterial toxicological assay of calcium oxide nanoparticles against some plant growth-promoting rhizobacteria. Int. J. Res. Appl. Sci. Eng. Technol.2018, 6: 460-466.
14. Alwash, A. The Green synthesis of zinc oxide catalyst using pomegranate peels extract for the photocatalytic degradation of methylene blue dye; Baghdad Scie. J.2020; 17(3):787-794.
15. Bala, N., Saha, S., Chakraborty, M., Maiti, M., Das, S. Nandy, Green synthesis of zinc oxide nanoparticle using *Hibiscus subdariffa* leaf extract: Effect of temperature on synthesis, antibacterial activity, and antidiabetic activity. RSC Adv. 2015; 5:4993-5003.
16. Abadi A. H., Al-Abodi, E. E. A review article: Green synthesis by using different plants to prepare oxide nanoparticles; IHJPAS. 2023; 36(1):56-63.
17. Ali Salman, R. Histopathological effect of zinc oxide nanoparticles on kidney and liver tissues in albino male mice; Ibn Al-Haitham J. Pure and Appl. Sci. 2018;13 (3):35-44.
18. Mostafa, M., Alrowaili, A., Al Shehri, M. Structural and optical properties of calcium titanate prepared from gypsum; J. Nanotechnology.2022; Article ID 6020378, 9 pp.
19. Kumar, A., Jha, S., Kumar, A., Kumar, S. Innovative investigation of zinc oxide nanoparticles used in dentistry. Crystals. 2022; 12(8):1063-1074.
20. AL-Dhahir, T.A., Entisar AL-Abodi, E., Tagreed. M. ZnO nanoparticles: Synthesis and crystal structure study. Wasit J. Sci. and Med. 2014;7(3):87-95.
21. Jayaram Babu, N., Kumari, S., Rao, K., Prabhu, Y. Germination and growth characteristics of mungbean seeds (*Vignaradiata* L.) affected by synthesized zinc oxide nanoparticles. Int. J. Curr. Eng. Technol. 2014; 4: 3411-3416.
22. Ahlaam, J., Entisar Al-Abodi, E., Bushra Hussein, H. Investigation of the optical and electrical properties of composites of PVA-PVP-PEG/ZnO Nanoparticles. J. Eng. Applied Sci. 2019; 14(16): 5819-5826.
23. Melo, M., Guedes, S., Xu, H., Rodrigues, L. Nanotechnology-based restorative materials for dental caries management. Trends Biotechnol. 2013;31:459-467.
24. Samiei, M., Torab, A., Hosseini, O., Abbasi, T., Ardalan Abdollahi, A. Divband, B. Antibacterial effect of two nano zinc oxide gel preparations compared to calcium hydroxide and chlorhexidine mixture. Iran Endod J. 2018;13(3):305-331.
25. Souza Aguiar, A. Guerreiro-Tanomaru, G. Faria, R. Toledo Leonardo, M. Tanomaru-Filho, J. M. Antimicrobial activity and pH of calcium hydroxide and zinc oxide nanoparticles intracanal medication and association with chlorhexidine. The J. Contemporary Dental Practice. 2015;16(8):624-629.